



A VERTICAL CHANNEL WITH OSCILLATORY TEMPERATURES AND CONCENTRATIONS AND VARIATION IN QUADRATIC DENSITY TEMPERATURE HAS AN EFFECT ON DISTURBING HEAT CONVULSION AND MASS TRANSFER FLOW

Dr Kanoth MaithiliKiranmai

Department of H&S in G.Pullaiah College of Engineering & Technology (AUTONOMOUS)

Email-Id: kanothmai1284@gmail.com

ABSTRACT

We examine how a porous medium's flow with unstable convectional heat and mass transfer changes with quadratic density temperature in a vertical slit with walls that are continuously oscillating in temperature and substance concentration. After the governing equations are resolved, different changes to the governing parameters are examined.

Keywords

Convective transmission of mass and heat, Quadratic density, Oscillatory Temperature, Vertical Channel.

1. INTRODUCTION

The domains of chemical engineering, aviation, and the production of nuclear energy, free convection is widely used as a means of heat transmission. Due to its engineering uses, free convection, which has been extensively researched in the disciplines of nuclear power plants,, thermal exchangers, and air conditioning systems in thermionic devices, An analysis of the asymmetric heating and cooling of two parallel vertical walls that causes a transitory The viscous, incompressible fluid between them is moving freely by convection. The flow might become unstable for many different reasons. Periodic heat inputs exist when an ac voltage that has been partially rectified or on/off control mechanisms have caused the current to be periodic. (4,6,7,8,12).

Natural convection flow is a common occurrence in many natural phenomena and has many industrial uses. It is caused by the simultaneous action of thermal and solenoidal buoyancy forces acting on the movement of a small Prandtl number fluid with a high gravitational force sensitivity and different geometries in a fluid with a porous medium. Understanding Parallel plate channels exhibit natural convection, which is crucial for a variety of real-world applications, such as analysing heat transfer from numerous printed circuit boards that are stacked parallel to one another or heat exchange in radiators that use massive parallel fins. Based on their orientation, these parallel plate channels are classified as vertical: The fluid flow in this direction is established by buoyancy force, which only acts in the vertical direction. Inclined: Strong secondary flows exploited in formation are caused by the buoyancy force's two components, normal and stream-wise. (1, 2, 3, 5, 9, 10, 11).

2.CONCEPT OF THE PROBLEM

The erratic flow of a thick, impermeable liquid through a porous material in a vertical duct with flat sides is what we are thinking about here. The fluctuating temperature and concentration that are mandated on the boundaries are what cause the flow to be unsteady. In a Cartesian coordinate system $0(x, y)$ with walls at $y = \pm 1$, the Boussinesq approximation is used to easily account for the density variation on the buoyancy component. Kinematic viscosity ν and thermal conductivity k are also constants. The flow and heat transfer equations are as follows.

$$\frac{\partial u}{\partial t} = \frac{\mu}{\rho} \frac{\partial^2 u}{\partial y^2} - \left(\frac{\mu}{k}\right)u - \rho \bar{g} \quad (1)$$

$$\rho_0 C_p \frac{\partial T}{\partial t} = K_f \frac{\partial^2 T}{\partial y^2} - Q(T - T_0) + 2\mu(u_y^2) + \frac{\mu}{k}u^2 \quad (2)$$

$$\frac{\partial C}{\partial t} = D_1 \frac{\partial^2 C}{\partial y^2} - KC \quad (3)$$

$$\rho - \rho_o = -\beta_o(T - T_o) - \beta_1(T - T_o)^2 - \beta^*(C - C_o) \quad (4)$$

where T, C, and u are the temperature, T is a velocity component in the x-direction, concentration, density, k_f coefficient of heat conductivity, coefficient of volume expansion, dynamic viscosity Q measures how powerful a heat source is, and

The molecular diffusivity is D1.

These define the border circumstances.

$$y = \pm L$$

$$u = 0, T = T_1, C = C_1,$$

$$u = 0, T = T_1 + \epsilon(T_2 - T_1) \cos(\omega t), C = C_1 + \epsilon(C_2 - C_1) \cos(\omega t) \quad (2.4)$$

Equations (1) and (2), when the dashes are removed, become

$$\gamma_1^2 \frac{\partial u}{\partial t} = G(\theta + \gamma \theta^2 + N\phi) + \frac{\partial^2 u}{\partial y^2} - (D^{-1} + M^2)u \quad (5)$$

$$P\gamma_1^2 \frac{\partial \theta}{\partial t} = \frac{\partial^2 \theta}{\partial y^2} - \alpha \theta + PE_c u_y^2 + PE_c D^{-1} u^2 \quad (6)$$

$$Sc\gamma_1^2 \frac{\partial \phi}{\partial t} = \frac{\partial^2 \phi}{\partial y^2} - \gamma_2 \phi \quad (7)$$

Where

$$G = \beta g L^3 \frac{(T_2 - T_1)}{\gamma^2} \quad (\text{Grashof number}) \quad D^{-1} = \frac{L^2}{k} \quad (\text{Darcy parameter})$$

$$P = \frac{\mu C_p}{K_f} \quad (\text{Prandtl number}) \quad Ec = \frac{\mu}{\Delta T C_p} \quad (\text{Eckert Number})$$

$$\alpha = \frac{Q \cdot L^2}{K_f} \quad (\text{Heat source parameter}) \quad N = \frac{4\sigma^* T_e^3}{3\beta_R} \quad (\text{Radiation parameter})$$

$$\gamma^2 = \frac{\omega L^2}{\nu} \quad (\text{Wormsely Number}) \quad P_1 = \frac{3NP}{3N+4} \quad \alpha_1 = \frac{3N\alpha}{3N+4}$$

$$M_1^2 = D^{-1}$$

The steady and transient terms are separated in equations 5 and 6

$$\frac{\partial^2 u_0}{\partial y^2} - M_1^2 u_0 = -G(\theta_0 + N\phi_0 + \gamma\theta_0^2) \quad (8)$$

$$\frac{\partial^2 u_1}{\partial y^2} - (M_1^2 + i\gamma^2)u_1 = -G(\theta_1 + N\phi_1 + 2\theta_0\theta_1) \quad (9)$$

$$\frac{\partial^2 \theta_0}{\partial y^2} - \alpha_1 \theta_0 + P_1 Ec \frac{\partial^2 u_0}{\partial y^2} + P_1 Ec D^{-1} u_0^2 = 0 \quad (10)$$

$$\frac{\partial^2 \theta_1}{\partial y^2} - (\alpha_1 + iP\gamma^2)\theta_1 + (2P_1 Ec) \frac{\partial u_0}{\partial y} \cdot \frac{\partial u_1}{\partial y} + (P_1 Ec D^{-1})u_0 u_1 \quad (11)$$

$$\frac{\partial^2 \phi_0}{\partial y^2} - \gamma_2 \phi_0 = 0 \quad (12)$$

$$\frac{\partial^2 \phi_1}{\partial y^2} - (\gamma_2 + iSc\gamma_1^2)\phi_1 = 0 \quad (13)$$

comparable terms in equations (8-13), we obtain

$$u_{00}^{11} - M_1^2 u_{00} = -G(\theta_{00} + N\phi_{00} + \gamma\theta_{00}^2), u_{00}(\pm 1) = 0 \quad (14)$$

$$\theta_{00}^{11} - \alpha_1 \theta_{00} = 0, \quad \theta_{00}(-1) = 0, \theta_{00}(+1) = 1 \quad (15)$$

$$\phi_{00}^{11} - \gamma_2 \phi_{00} = 0, \quad \phi_{00}(-1) = 0, \phi_{00}(1) = 1$$

$$u_{01}^{11} - M_1^2 u_{01} = -G(\theta_{01} + N\phi_{01}), u_{01}(\pm 1) = 0 \quad (16)$$

$$\theta_{01}^{11} - \alpha_1 \theta_{01} = -P_1 u_{00}^{12} - P_1 D^{-1} u_{00}^2, \quad \theta_{01}(-1) = 0 = \theta_{01} \quad (17)$$

$$\phi_{01}^{11} - \gamma_2 \phi_{01} = 0, \quad \phi_{01}(-1) = 0 = \phi_{01}(+1)$$

$$u_{10}^{11} - (M_1^2 + i\gamma^2)u_{10} = -G(\theta_{10} + N\phi_{10}), u_{10}(\pm 1) = 0 \quad (18)$$

$$\theta_{10}^{11} - iP_1 \gamma^2 \theta_{10} = 0, \quad \theta_{10}(-1) = 0, \quad \theta_{10}(+1) = 1 \quad (19)$$

$$\theta_{10}^{11} - iP_1 \gamma^2 \theta_{10} = 0$$

$$u_{11}^{11} - (M_1^2 + i\gamma^2)u_{11} = -G(\theta_{11} + N\phi_{11}), u_{11}(\pm 1) = 0 \quad (20)$$

$$\theta_{11}^{11} - (\alpha_1 + iP_1 \gamma^2)\theta_{11} = -2P_1 u_{00}^1 u_{10}^1 - 2P_1 D^{-1} u_{00} u_{10}, \quad \theta_{11}(\pm 1) = 0 \quad (21)$$

3. SHEAR STRESS NUSSELT NUMBER

$$\tau = \mu \left(\frac{du}{dy} \right)_{\pm L}$$

NUSSELT NUMBER

$$Nu(\pm 1) = \left(\frac{d\theta}{dy} \right)_{y=\pm 1}$$

4. Examine Of the Conclusion

We explore the impact of chemical reactions, thermo-diffusion, and quadratic density-temperature fluctuations discusses a viscous dissipative fluid's mass and heat transmission by convection occurs in a horizontal duct with varying thermodynamics and concentration. It is discussed how differences in G, M, γ , γ_1, γ_2 , Sc, S0, Ec, N, and α . affect velocity, temperature, and concentration. The axial velocity u represents the change of u with Grashof number G and is displayed in Fig. 1. In the case of $G > 0$ and G_0 , it is found that u is in the vertical and upward directions, respectively. |G| raises |u| across the whole flow zone, with $y = 0.4$ experiencing the greatest boost. According to the fluctuation of u with Hartman number M, the following region (fig 2) has smaller |u| values the greater the Lorentz force. The distribution of temperatures that are not dimensions (θ) is represented by Sc (fig 3). The real temperature in the flow zone is inversely correlated with molecular diffusivity. Fig 4 illustrates the impact of thermo diffusion. The real temperature in the flow zone decreases with $S_0 > 0$ and increases with $|S_0|$. This diagram displays the non-dimensional concentration (C). When buoyancy forces work in opposition to one another, the flow area expands and the actual concentration drops (fig.5). This occurs when molecular buoyancy force outweighs thermal buoyancy force. (fig.6) shows how the heat source

influences C. It shows how raising the concentration causes a rise in the actual concentration.

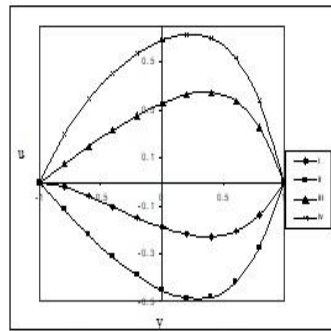


Fig.1 Variation of u with G

$M=2, \alpha=2, N=1, S_c=1.30, S_0=50, E_c=0.1, \gamma=0.5, \gamma_1=0.5 \& \gamma_2=0.5$

G	I	II	III	IV
	2×10^3	4×10^3	-2×10^3	-4×10^3

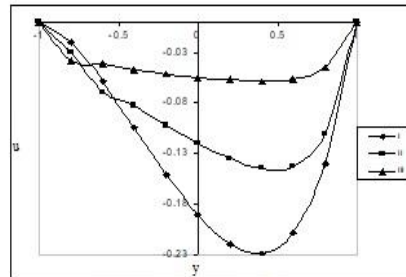


Fig.2 Variation of u with M

$G=2 \times 10^3, \alpha=2, N=1, S_c=1.30, S_0=50, E_c=0.1, \gamma_1=0.5 \& \gamma_2=0.5$

M	I	II	III
	2	4	6

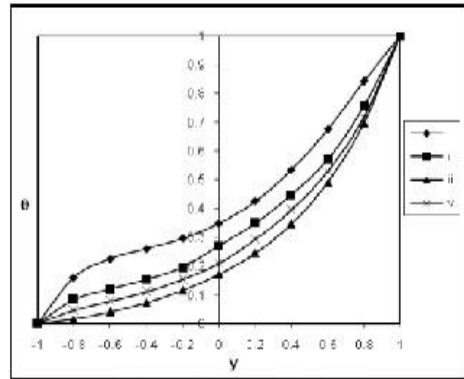


Fig.3 Variation of θ with S_c

$G=2 \times 10^3, M=2, \alpha=2, N=1, S_0=50, E_c=0.1, \gamma_1=0.5 \& \gamma_2=0.5$

S_c	I	II	III	IV
	0.2	0.6	1.3	2

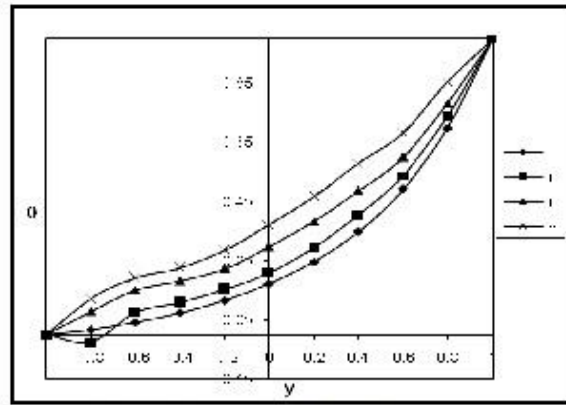


Fig. 4 Variation of θ with S_0
 $G=2 \times 10^3, M=2, \alpha=2, N=1, S_C=1.30, E_C=-0.01, \gamma_1=0.5$ & $\gamma_2=0.5$

	I	II	III	IV
S_0	0.5	1	-0.5	-1

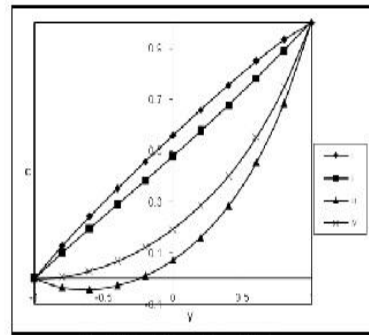


Fig. 5 Variation of c with N
 $G=2 \times 10^3, M=2, N=1, S_C=1.30, S_0=50, E_C=-0.01, \gamma_1=0.5$ & $\gamma_2=0.5$

	I	II	III	IV
N	1	2	-0.5	-0.8

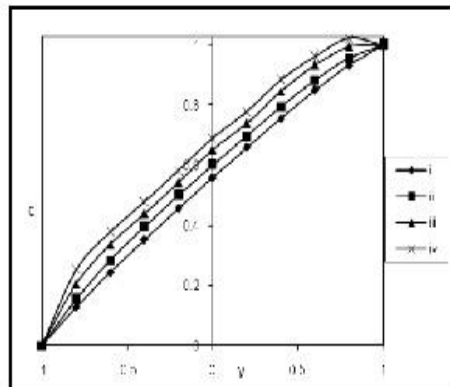


Fig. 6 Variation of c with α
 $G=2 \times 10^3, M=2, N=1, S_C=1.30, S_0=50, E_C=-0.01, \gamma_1=0.5$ & $\gamma_2=0.5$

	I	II	III	IV
α	2.5	4.5	5.5	6.5

5. Tables

Due to differences in D^{-1} , M , γ , γ_1, γ_2 , S_c, S_0, N and α the stress (τ) at $y = 1$, see tables (1-5). By increasing $|G|$, γ and M at both walls, the shear stress was enhanced. As the τ α stress changes, the growth in $\alpha \leq 4$ and depreciation in $\alpha \leq 6$ are both enhanced. The fluctuation of γ_1 and γ_2 demonstrates that as $y = 1$ and $y = +1$ grow, so do the Wormesly numbers γ_1 and $\gamma_1 \geq 0.7$, and as $y = +1$ increases, so does the magnitude of $|\tau|$. The component of the chemical reaction $\gamma_2 \leq 2.5$ enhances $|\tau|$ and diminishes greater $\gamma_2 \geq 3.5$ at $y = 1$. According to the variation with Sc , the lower the diffusivity of molecules, the smaller $|\tau|$ for the greater $|\tau|$ the walls, both reduction in diffusivity. Additionally, at $y = -1$, $|\tau|$ improves as $|S_0|$ rises. When molecular In the same direction, buoyancy forces operate and decrease in size when they act in the opposite direction, respectively, the stress at both walls rises, according to the fluctuation in buoyancy ratio N . When Ec is positive for $G > 0$ and negative for G_0 , $|\tau|$ appreciates. For every G , this variation is accurate.

Tables (6–10) display, for various parametric values, temperature change speed (Nu) at $y = \pm 1$. The heat flux transmission is discovered to $y = +1$ increase with $|G|$ and M and degrade at γ . The heat flux transmission at $y = 1$ accelerates with $\alpha < 4$ according to the Nu value's variation with the heat source parameter. Tables display the Nu variation when γ_1 and γ_2 are used. The rise in the chemical reaction parameter γ_2 is observed to boost $|Nu|$ at $y = +1$, diminish with $\gamma_2 \leq 1.5$, and enhance with $\gamma_2 \geq 2.5$. Additionally, for $y = +1$, a rise in 1 improves $|Nu|$, and $\gamma_1 \geq 0.5$ causes $|Nu|$ to fall. The fluctuation of Nu with Sc demonstrates that, for every G , a bigger $|Nu|$ is present at $y = -1$ for a further decrease in diffusivity, which reduces the rate of heat transfer. The rate of heatsensor at $y = -1$ is enhanced $|S_0|$ while it is decreased by an increase in $S_0 > 0$. The rate of heat transfer increases when both upward forces are operating in the same direction, and it decreases when the molecular upward force exceeds power of thermal buoyancy when $y = -1$. Change of Nu with Ec shows that it decreases with $Ec \leq 0.03$ and increases with $Ec \geq 0.05$ at $y = 1$.

Table (11–14), the Sherwood number (Sh) at $y = \pm 1$ is examined. It constructs the mass transfer rate more effectively at $y = +1$ and depreciates at $y = -1$ in G . $|Sh|$ rises and falls when the density ratio rises at $y = +1$ and $y = -1$, respectively. Additionally, $|Sh|$ decreases when $y = \pm 1$ due to the Wormesly number increasing by γ_1 . With $S_0 > 0$, $|Sh|$ drops at $y = -1$ and enhances at $y = +1$, whereas it enhances at both walls $|S_0|$, Sh with chemical reaction parameter γ_2 demonstrates that Sh increase in $\gamma_2 \leq 2.5$ and reduces $\gamma \geq 3.5$. At $y = +1$, higher dissipative heat results in smaller $|Sh|$; at $y = -1$, larger dissipative heat results in smaller $|Sh|$. $|Sh|$ grows at $y = +1$ and declines at $y = -1$, increases in $N > 0$ and reduces with $|N|$, according to the fluctuation of sh with N .

Table 1
Shear stress (τ) at $r = 1$
 $\alpha=2.5, \gamma_1=0.5, \gamma_2=0.5, S_c=1.30, S_0=0.5, N=1, E_c=0.01$

G	I	II	III	IV	V
10^3	0.63748	1.07964	1.38543	0.93306	0.93406
3×10^3	1.21304	1.45572	2.33044	1.30106	1.30206
-10^3	-1.28087	-0.73184	-1.30517	-1.28087	-1.29087
-3×10^3	-1.64886	-1.10792	-2.25017	-1.64886	-1.66886
M	2	4	6	2	2
γ	0.5	0.5	0.5	1.5	2.5

Table 2
Shear stress (τ) at $r = 1$
 $M=2, \gamma=0.5, \gamma_1=0.5, \gamma_2=0.5, S_c=1.30, S_0=0.5, N=1, E_c=0.01$

G	I	II	III
10^3	0.63748	2.70735	1.50421
3×10^3	1.21304	3.18485	1.90032
-10^3	-1.28087	-2.12693	-1.48554
-3×10^3	-1.64886	-3.26758	-2.00676
α	2.5	4.5	6.5

Table 3
Shear stress (τ) at $r = 1$
 $M=2, \gamma=0.5, \alpha=2.5, S_c=1.30, S_0=0.5, N=1, E_c=0.01$

G	I	II	III	IV	V	VI	VII
10^3	0.63748	1.07218	0.47452	0.86350	1.36285	-0.08254	-4.41434
3×10^3	1.21304	2.29975	1.63467	1.23150	2.16063	0.59011	1.16837
-10^3	-1.28087	-1.57173	-1.21131	-1.35043	-1.18255	3.43148	2.4355
-3×10^3	-1.64886	-2.63337	-1.57930	-1.71842	-2.77249	-2.78628	1.7865
γ_1	0.5	0.1	0.5	0.7	0.5	0.5	0.5
γ_2	0.5	0.5	0.5	0.5	1.5	2.5	3.5

Table 4
Shear stress (τ) at $r = -1$
 $M=2, \gamma=0.5, \alpha=2.5, \gamma_1=0.5, \gamma_2=0.5, N=1, E_c=0.01$

G	I	II	III	IV	V	VI	VII
10^3	-20.4569	-1.95718	0.34982	0.46221	0.63880	2.21977	3.62307
3×10^3	-30.10370	2.67626	0.10880	-0.80656	1.42117	3.78562	5.27196
-10^3	-15.20341	-0.50139	0.6466	0.66886	-7.32593	-2.03780	-3.08903
-3×10^3	-29.54091	-0.38187	0.51326	1.42117	-1.50551	-2.81149	-4.47387
S_c	0.24	0.6	1.30	2.01	1.30	1.30	1.30
S_0	0.5	0.5	0.5	0.5	1.0	-0.5	-1.0

Table 5

Shear stress (τ) at $r = -1$

$M=2, \gamma=0.5, \alpha=2.5, \gamma_1=0.5, \gamma_2=0.5, S_c=1.30, S_0=0.5$

G	I	II	III	IV	V	VI	VII
10^3	0.34982	1.24600	1.29037	1.46285	0.68309	1.11943	1.02324
3×10^3	0.10880	0.27772	0.48673	0.63169	0.36019	1.03482	1.00528
-10^3	0.6466	-0.40782	-0.28030	-0.15278	0.02699	-4.0935	-0.31316
-3×10^3	0.51326	0.36830	0.22334	0.07838	0.43799	-4.3477	0.51326
E_c	0.01	0.03	0.05	0.07	0.01	0.01	0.01
N	1	1	1	1	2	-0.5	-0.8

Table 6

Nusselt number (Nu) at $r = 1$

$\alpha=2.5, \gamma_1=0.5, \gamma_2=0.5, S_c=1.30, S_0=0.5, N=1, E_c=0.01$

G	I	II	III	IV	V
10^3	1.88527	2.87179	19.61565	1.86445	1.80445
3×10^3	2.7779	6.67923	73.65454	2.73533	2.70533
-10^3	1.89445	2.87179	19.61565	1.86445	1.82445
-3×10^3	2.73533	6.67923	73.65454	2.70533	2.66533
M	2	4	6	2	2
γ	0.5	0.5	0.5	1.5	2.5

Table 7

Nusselt number (Nu) at $r = 1$

$M=2, \gamma=0.5, \gamma_1=0.5, \gamma_2=0.5, S_c=1.30, S_0=0.5, N=1, E_c=0.01$

G	I	II	III
10^3	1.88527	3.28585	2.61149
3×10^3	2.7779	3.18485	2.68301
-10^3	1.89445	2.30302	2.60656
-3×10^3	2.73533	3.06881	2.68339
α	2.5	4.5	6.5

Table 8
Nusselt number (Nu) at $r = 1$
 $M=2, \gamma=0.5, \alpha=2.5, S_c=1.30, S_0=0.5, N=1, E_c=0.01$

G	I	II	III	IV	V	VI	VII
10^2	2.18527	1.89445	1.99095	2.29445	1.53398	0.69111	2.76604
3×10^2	2.7779	1.29432	2.73445	2.93533	1.29432	-2.06272	1.13102
-10^2	1.99445	1.53398	1.89445	2.19445	1.53057	2.14225	3.4569
-3×10^2	2.88533	1.29347	2.73533	2.93533	1.29347	-1.69994	2.1245
γ_1	0.5	0.1	0.5	0.7	0.5	0.5	0.5
γ_2	0.5	0.5	0.5	0.5	1.5	2.5	3.5

Table 9
Nusselt number (Nu) at $r = -1$
 $M=2, \gamma=0.5, \alpha=2.5, \gamma_1=0.5, \gamma_2=0.5, N=1, E_c=0.01$

G	I	II	III	IV	V	VI	VII
10^2	-40.2169	-0.64645	-0.99901	-1.27456	-0.37688	0.10916	0.11862
3×10^2	-54.40278	-0.76328	-1.15383	-1.46055	-0.90235	0.03447	0.14927
-10^2	-13.51371	-0.06383	-0.99641	-1.26589	-0.37492	0.07797	0.08867
-3×10^2	-54.55033	-0.61763	-1.13364	-1.45838	-0.90186	0.02667	0.14429
S_c	0.24	0.6	1.30	2.01	1.30	1.30	1.30
S_0	0.5	0.5	0.5	0.5	1.0	-0.5	-1.0

Table 10
Nusselt number (Nu) at $r = -1$
 $M=2, \gamma=0.5, \alpha=2.5, \gamma_1=0.5, \gamma_2=0.5, S_c=1.30, S_0=0.5$

G	I	II	III	IV	V	VI	VII
10^2	-0.99901	-0.86623	-1.30554	-1.88139	-0.50179	-0.16536	-0.12863
3×10^2	0.15383	-3.29155	-5.51841	-7.77942	-2.38682	-1.04597	-0.89461
-10^2	0.99641	-0.72968	-1.30554	-1.88139	-1.50179	-0.16536	-0.12863
-3×10^2	-1.13364	-0.09541	-5.51841	-7.77942	-2.38823	-1.04254	-0.99641
E_c	0.01	0.03	0.05	0.07	0.01	0.01	0.01
N	1	1	1	1	2	-0.5	-0.8

Table 11
Sherwood number (Sh) at $r = 1$
 $\alpha=2.5, N=1, E_c=0.01, S_0=0.5$

G	I	II	III	IV	V	VI	VII	VIII	IX	X	XI
10^2	0.26233	0.29071	0.2849	0.2529	0.2345	0.7243	1.8881	1.7999	0.70916	0.5671	0.0104
3×10^2	0.29071	0.3212	0.3052	0.2612	0.2409	0.8942	1.2452	1.5249	0.7249	0.6409	0.0256
γ	0.5	1.5	2.5	0.5	0.5	0.5	0.5	0.5	0.5	0.5	0.5
γ_1	0.5	0.5	0.5	0.1	0.3	0.5	0.5	0.5	0.5	0.5	0.5
γ_2	0.5	0.5	0.5	0.5	0.5	1.5	2.5	3.5	0.5	0.5	0.5
S_c	1.3	1.3	1.3	1.3	1.3	1.3	1.3	1.3	0.24	0.6	2.01

Table 12
Sherwood number (Sh) at $r = 1$
 $\gamma=0.5, \gamma_1=0.5, \gamma_2=0.5, S_c=1.3$

G	I	II	III	IV	V	VI	VII	VIII	IX	X	XI	XII
10^2	0.2623	0.2225	1.3171	1.8303	0.3196	0.3485	0.3775	0.5473	1.8304	1.4454	0.1255	-0.0029
3×10^3	0.2909	0.2509	1.4212	1.5469	0.3696	0.4257	0.4926	0.6409	1.9521	1.5409	0.1609	-0.0125
S_0	0.5	1	-0.5	-1	0.5	0.5	0.7	0.5	0.5	0.5	0.5	0.5
Ec	0.01	0.01	0.01	0.01	0.03	0.05	0.07	0.01	0.01	0.01	0.01	0.01
N	1	1	1	1	1	1	1	2	-0.5	-0.5	1	1
α	2	2	2	2	2	2	2	2	2	2	4	6

Table 13
Sherwood number (Sh) at $r = -1$
 $\alpha=2.5, N=1, Ec=0.01, S_0=0.5$

G	I	II	III	IV	V	VI	VII	VIII	IX	X	XI
10^2	0.72168	0.68681	0.5849	0.68681	0.5829	0.37021	0.89677	0.5666	0.43124	0.51804	0.8572
3×10^3	0.6868	0.5892	0.520	0.3702	0.328	0.3098	0.8059	0.508	0.1597	0.2592	0.752
γ	0.5	1.5	2.5	0.5	0.5	0.5	0.5	0.5	0.5	0.5	0.5
γ_1	0.5	0.5	0.5	0.1	0.3	0.5	0.5	0.5	0.5	0.5	0.5
γ_2	0.5	0.5	0.5	0.5	0.5	1.5	2.5	3.5	0.5	0.5	0.5
Sc	1.3	1.3	1.3	1.3	1.3	1.3	1.3	1.3	0.24	0.6	2.01

Table 14
Sherwood number (Sh) at $r = -1$
 $\gamma=0.5, \gamma_1=0.5, \gamma_2=0.5, S_c=1.3$

G	I	II	III	IV	V	VI	VII	VIII	IX	X	XI
10^3	0.72168	1.0024	0.0599	-0.254	0.70791	0.7291	0.7501	0.5301	-0.254	0.0184	0.8853
3×10^3	0.6868	0.8524	0.0382	-0.153	0.6256	0.6496	0.7056	0.4692	-0.23	-0.009	1.0356
S_0	0.5	1	-0.5	-1	0.5	0.5	0.7	0.5	0.5	0.5	0.5
Ec	0.01	0.01	0.01	0.01	0.03	0.05	0.07	0.01	0.01	0.01	0.01
N	1	1	1	1	1	1	1	2	-0.5	-0.5	1
α	2	2	2	2	2	2	2	2	2	4	6

6. RESOURCES:

- 1) Anug W (1972). *Int. J. Heat and Mass Transfer*.
- 2) Campo A, Manca O, and Marrone B, *ASME Journal of Applied Mechanics*.
- 3) Gill W, M and Casal, A.D *Inst.Chem. Engg. Jour*.
- 4) Jha BK, Singh AK, and Takhar HS (*International Journal of Applied Mechanics and Engineering*).
- 5) Manca O, Marrone B, Nardini S, and Naso V, In: Sunden B, Comini G. *Computational Analysis of Convection Heat Transfer*. WIT Press, Southampton.
- 6) Narahari M, Sreenadh S, and Soundalgekar VM *Thermophysics and Aeromechanics*,

- 7) Narahari M *.Proceedings of International Conference on Mechanical & Manufacturing Engineering .*
- 8) Narahari M. *Int. J. of Appl. Math. And Mech.*
- 9) Ostrach S Technical Report 2863, NASA, USA.
- 10) Ostrach S Technical Report 3141, NASA, USA.
- 11) Pantokratoras A *ASME Journal of Heat Transfer.*
- 12) Singh AK and Paul T *,International Journal of Applied Mechanics and Engineering.*